PLOS ONE

RESEARCH ARTICLE

# Mapping Spatial Variability of Soil Salinity in a Coastal Paddy Field Based on Electromagnetic Sensors

**Yan Guo[1,2], Jingyi Huang[3], Zhou Shi[1]*, Hongyi Li[4]**

**1** Institute of Agricultural Remote Sensing and Information Technology Application, College of Environmental and Resource Sciences, Zhejiang University, Hangzhou, China, **2** Institute of Agricultural Economics and Information, Henan Academy of Agricultural Sciences, Zhengzhou, China, **3** School of Biological, Earth and Environmental Science, The University of New South Wales, Kensington, NSW 2052, Australia, **4** School of Tourism and Urban Management, Jiangxi University of Finance and Economics, Nanchang, China

* shizhou@zju.edu.cn





**Citation:** Guo Y, Huang J, Shi Z, Li H (2015) Mapping Spatial Variability of Soil Salinity in a Coastal Paddy Field Based on Electromagnetic Sensors. PLoS ONE 10(5): e0127996. doi:10.1371/journal.pone.0127996

**Academic Editor:** Inés Álvarez, University of Vigo, SPAIN

**Received:** January 3, 2015

**Accepted:** April 21, 2015

**Published:** May 28, 2015



**Data Availability Statement:** All relevant data are within the paper and its Supporting Information files.

**Funding:** This research was supported by National Natural Science Foundation of China (No. 41271234; No. 41101197), the National High-tech R&D Program of China (No.2013AA102301), the Key National Projects of High-Resolution Earth Observing System (09-Y30B03-9001-13/15) and by the Independent Innovative Project of Henan Academy of Agricultural Sciences. The funders had no role in study design, data collection and analysis, decision to publish, or preparation of the manuscript.

## Abstract

In coastal China, there is an urgent need to increase land area for agricultural production and urban development, where there is a rapid growing population. One solution is land reclamation from coastal tidelands, but soil salinization is problematic. As such, it is very important to characterize and map the within-field variability of soil salinity in space and time. Conventional methods are often time-consuming, expensive, labor-intensive, and unpractical. Fortunately, proximal sensing has become an important technology in characterizing within-field spatial variability. In this study, we employed the EM38 to study spatial variability of soil salinity in a coastal paddy field. Significant correlation relationship between $EC_a$ and $EC_{1:5}$ (i.e. $r > 0.9$) allowed us to use EM38 data to characterize the spatial variability of soil salinity. Geostatistical methods were used to determine the horizontal spatio-temporal variability of soil salinity over three consecutive years. The study found that the distribution of salinity was heterogeneous and the leaching of salts was more significant in the edges of the study field. By inverting the EM38 data using a Quasi-3D inversion algorithm, the vertical spatio-temporal variability of soil salinity was determined and the leaching of salts over time was easily identified. The methodology of this study can be used as guidance for researchers interested in understanding soil salinity development as well as land managers aiming for effective soil salinity monitoring and management practices. In order to better characterize the variations in soil salinity to a deeper soil profile, the deeper mode of EM38 (i.e., EM38v) as well as other EMI instruments (e.g. DUALEM-421) can be incorporated to conduct Quasi-3D inversions for deeper soil profiles.

## Introduction

Over the past decades, much of the tidelands in China have been reclaimed for agriculture and urban buffer zone [1]. However, the highly saline coastal soil often causes adverse effects on

**Competing Interests:** The authors have declared that no competing interests exist.

agricultural productivity, particularly in the first 20 years of agricultural production. After nearly 20 years of farming, the soil salinity has changed dramatically and the salts have leached into deeper soil profiles due to the irrigation farming and high level of precipitation across these coastal areas. In order to make profits from the reclaimed soils, farmers start to plant more profitable crops (e.g. rice) on the reclaimed lands. However, loss of yield often occurs because of the subjective diagnose of the salinity level of the reclaimed soils using farmers' experiences. In order to better management the reclaimed soils (especially salinity) within these coastal areas, it is important to characterize the spatial variations of soil salinity, especially within the root zone [2], in an accurate and efficient way.

Conventional soil salinity mapping has been done by visual observations with limited laboratory measurements (United States Salinity Laboratory Staff, 1954; Soil Survey Division Staff, 1993). However, visual observations provide only qualitative information [3] and laboratory methods are often time-consuming, expensive, and labor-intensive [4]. In order to quantify the soil variability using geostatistical methods, approximately 100 sample points are required to estimate a spatial statistical model [5]. For example, in an attempt to map soil salinity in a field in Southern Alberta Gallichand et al. [6] collected 80 soil samples at two different depths on a regular grid and used 2D- and 3D-kriging to interpolate the conductivity of the saturated paste extract (i.e., $EC_e$) of the study area.

The need for rapid, reliable, and easy-to-take measurements of soil salinity at field and landscape scales gave birth to the proximal sensing electromagnetic induction (EMI) [4]. EMI can produce a large number of georeferenced and quantitative measurements that can be easily correlated with the spatial variability of salinity [3]. The most commonly used conductivity meter (EM38, Geonics Ltd., Ont, Canada) measures soil apparent electrical conductivity ($EC_a$). The EM38 also has been used to map soil properties (e.g., $EC_e$ and soil moisture) using various calibration models [7–12] at field [10–11], region [13], and catchment [14] scales.

In addition to mapping the horizontal variability of soil salinity, a number of researchers have attempted to measure $EC_a$ at different depths with an inversion algorithm. A pioneering work in this field was undertaken by Hendrickx et al. [15]. They used Tikhonov regularization to invert the EM38 data using measurements collected at different heights above the ground and in different directions. Though successful, the inversion was essentially a 1-Dimension inversion and could not reflect the lateral variation of soil salinity. Several years later, researchers developed 2-Dimension inversion algorithms to invert the $EC_a$ data onto 2-D vertical slices and 2-D horizontal slices [16–18]. Most recently, a combination of vertical slices and horizontal slices was utilized to determine the 3-D variability of soil conductivity [19–21]. With these inversion approaches, spatial variability of soil electrical conductivity and the correlated soil properties (e.g. salinity) can be presented in a 2-D or 3-D view.

Despite the successful application of EMI in soil salinity mapping [19, 22–24], few studies have reported the use of EMI to determine temporal variability of soil salinity from a multi-dimensional view. The objective of this study is to map the spatio-temporal variability of soil salinity in a reclaimed costal paddy field using three years of EM38 data. Geostatistical analysis and a Quasi-3D inversion algorithm were combined to map the horizontal and vertical spatio-temporal variability of soil salinity in the study field.

## Materials and Methods

### Ethics Statement

We randomly chose 3 coastal paddy fields in the northern region of Shangyu City, Zhejiang Province, southeast of Hangzhou Bay, China and got permission from Agricultural Bureaus of Shangyu. One field (4.25 ha) was used to collect EM data in three consecutive years, and the

others were employed to collect validation data. These fields were the experimental fields in Zhejiang University. No endangered or protected species were involved in the study.

## Study Area

The study was conducted in a coastal saline area located in the northern region of Shangyu City, Zhejiang Province, southeast of Hangzhou bay, China. The climate is subtropical with an average annual temperature of 16.5°C. The average daily maximum and minimum monthly temperatures are 4°C (January) and 28°C (July), respectively. Average annual precipitation is 1300 mm, with the heaviest rainfall occurring during two rainy seasons between March and June and also during September. Over the past 40 years, approximately 17 000 ha of coastal land has been reclaimed around Shangyu City in successive programs (Fig 1A and 1B). The investigated fields were reclaimed in 1996. They were separated by small embankments (bunds) which ensured flooded conditions within each of the study fields. A photo of the study field is shown in Fig 1C.

## Data Collection and Processing

In the present study, an EM38proto (Geonics, Ltd., Ont., Canada) was used to record $EC_a$ data with a Geonics EM38 Data Logging System (DAS70-CX) and a field computer (Allegro CX). A

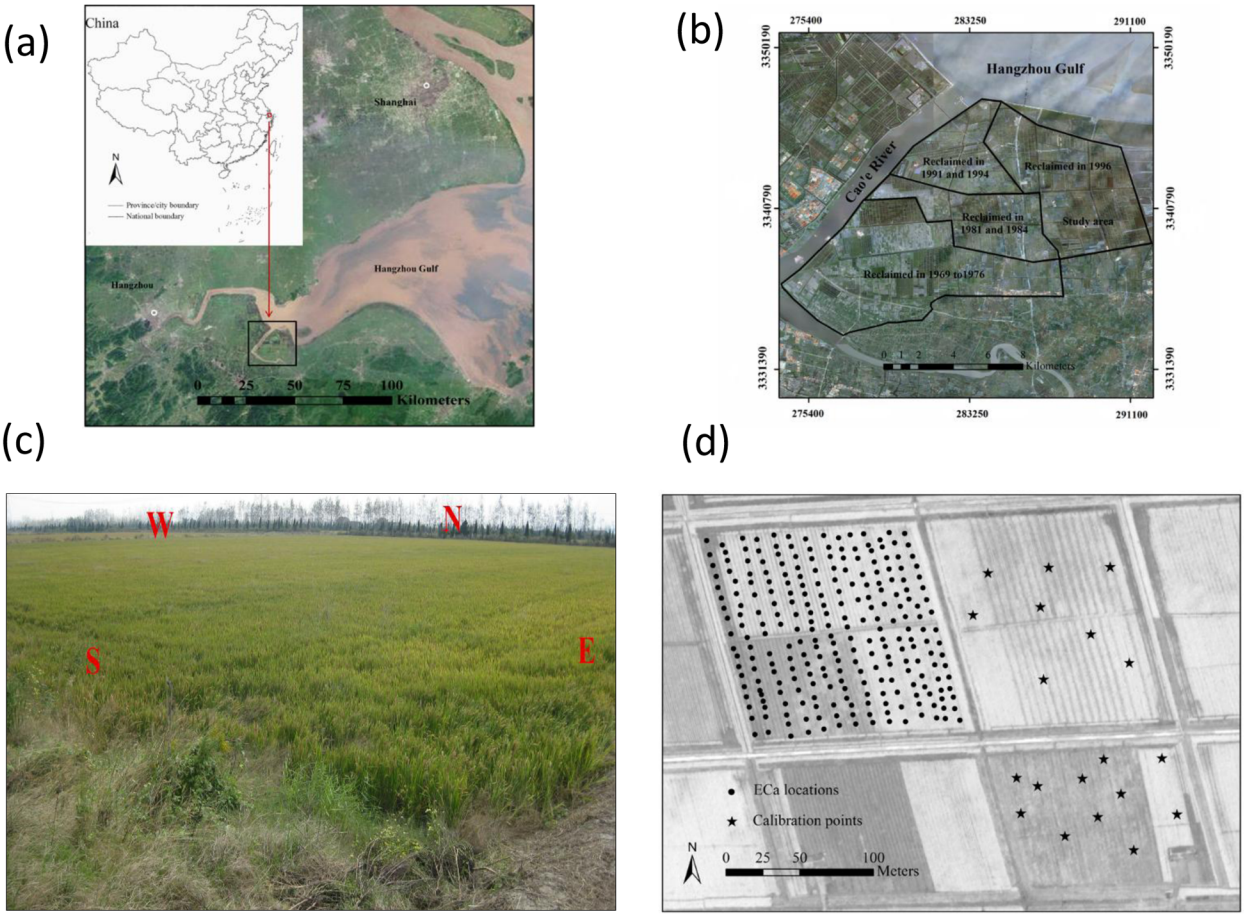


**Fig 1. Locations of the study field and $EC_a$ measurements.** (a) Location of the study field with reference to the Hangzhou Gulf, (b) reclaimed lands over the past 40 years; (c) A photo of the study field (Taken on October 2010) and (d) Location of $EC_a$ measurements in 2009 across the study area.

doi:10.1371/journal.pone.0127996.g001

separate Global Positioning System (GPS) with differential correction within 2 m was used for geo-reference.

In order to understand the correlation between soil salinity and $EC_a$ data, a preliminary EM38 survey was conducted in the adjacent fields to the east and southeast of the study field (Fig 1D). Afterwards, 19 soil cores were collected in these fields (Fig 1D) to a depth of 80 cm with a 20-cm interval (i.e. 0–20, 20–40, 40–60, 60–80 cm). The soils cores were selected to cover the different values of $EC_a$ measurements, including high (i.e. $EC_a \geq 300$ mS/m), medium (i.e. 200 mS/m$<EC_a<$300 mS/m) and low (i.e. $EC_a \leq 200$ mS/m) values. $EC_a$ measurements were recorded in the vertical (EM38v) and horizontal (EM38h) modes, respectively. Soil samples at various soil depths (i.e. 0–20 cm, 20–40 cm, 40–60 cm, 60–80 cm) were collected for lab analysis of soil salinity by a conventional conductivity meter using a 1:5 soil: water suspension ($EC_{1:5}$). Detailed information can be found in S1 File.

Subsequently, $EC_a$ measurements were taken along an approximate 20 m grid along the furrows in the study field (northwest of Fig 1D) in three consecutive years. There were 251, 256, and 339 $EC_a$ measurements collected in October 2009, November 2010, and November 2011, respectively. In order to calculate the coefficient of variation over time, EM38 measurements in 2010 and 2011 were harmonized onto a common grid consisting of the 251 $EC_a$ measurement sites in 2009 (See Fig 1D) using the nearest neighbor algorithm available in ArcGIS 9.3 (ESRI, 2013).

The $EC_a$ measurements were taken after the rice was harvested and the field was drained. According to Robinson et al. [25], EM38 measurements drift significantly when temperatures are over 40°C and the drift is more obvious for small $EC_a$ readings (i.e., less than 100 mS/m). Because the temperature conditions were similar when the three surveys were taken (approximately 25°C) and the study area was highly conductive, we did not calibrate the $EC_a$ measurements to a standard temperature of 25°C as suggested by Sheets and Hendrickx [26]. However, EM38 was calibrated according to the manual before the surveys to reduce the error [27–28].

## Characterizing Horizontal Spatio-Temporal Variability of Soil Salinity using Geostatistical Approaches

Geostatistical approaches are often used to define the variance structure, spatial distribution, and trend changes of soil properties. Ordinary kriging (OK) is one of the most popular interpolation methods [29]. The OK method uses a semivariogram to quantify the spatial variation of a regionalized variable [30]:

$$\gamma(h) = \frac{1}{2N(h)} \sum_{i=1}^{N(h)} [Z(x_i) - Z(x_i + h]^2) \quad (1)$$

where $\gamma(h)$ is a semivariogram that measures the mean variability between two points $x$ and $x + h$ as a function of their distance $h$; $Z(x_i)$ and $Z(x_{i+h})$ are the values of the variable $Z$ at location $x_i$ and $x_i+h$; $N(h)$ is the number of pairs of sample points separated by the lag distance $h$.

$EC_a$ measurements were interpolated by OK using Eq (2) [30] with ArcGIS 9.3 (ESRI, 2013) to calculate the horizontal spatial variability of soil salinity:

$$Z^*(x_0) = \sum_{i=1}^{n} \lambda_i Z(x_i) \quad (2)$$

where $Z^*(x_0)$ is the predicted $EC_a$ at location $x_0$; $Z(x_i)$ is the measured $EC_a$ at location $x_i$; $\lambda_i$ is the weight assigned to the observation $Z(x_i)$; and $n$ is the number of measurements.

With regard to the horizontal temporal variability, we calculated the coefficient of variation ($CVt_i$) over time at each measurement site to assess the stability of soil salinity (Eq 3). The technique has been used by Blackmore [31] to characterize the temporal stability of crop yields and by Shi et al. [32] to assess the stability of soil properties in grasslands.

$$CVt_i = \frac{\sqrt{(n \times \sum_{t=1}^{n} \mathrm{ECa}_{it}^2 - (\sum_{t=1}^{n} \mathrm{ECa}_{it}^2))/n \times n(n-1)}}{(\sum_{t=1}^{n} \mathrm{ECa}_{it}^2)/n} \quad (3)$$

Where $CVt_i$ is the coefficient of variation over three years at the $i$th ECa measurement site in the $t$th year and $n$ is the number of $EC_a$ measurements.

## Mapping Vertical Spatio-Temporal Variation in Soil Salinity Using Quasi-3D Inversion

In order to determine the distribution of true electrical conductivity (σ—mS/m) at different depths from the $EC_a$ measurements, an inversion software (EM4Soil) was used to convert $EC_a$ to σ. We employed the Quasi-3D module (Q3Dm) of the software following the procedure of Monteiro Santos et al. [33] to invert the $EC_a$ data of the three consecutive years. Q3Dm is a 1-Dimensional Spatial Constrained technique (1-D SCI) and a forward modeling approach. It assumes that below each measured site the 1-Dimension variation of the soil conductivity is constrained by the variation under neighboring sites. The modeling process is based upon the cumulative function [27]. The inversion algorithm is based on the Occam regularization method [34–35].

As the software requires standard grid files for inversion, gridding was applied onto the raw data set using the Gridding Tool of the Q3Dm package. The gridding was based on the inverse distance weighted method (EM4SOIL Manual, 2011). In this study, a weight value of 2.0 was selected and the grid consisted of 10 x-lines (west-east) and 8 y-lines (south-north) with grid spacing of 18 m.

After gridding, inversion of $EC_a$ data was performed using Algorithm 3 (designed for inversion of electromagnetic induction signal from single sensor) with a damping factor of 0.3, 10 iterations, a data error of 1.00, and a misfit target of 0.20. An initial 2-layer laterally homogeneous model was predefined with initial electrical conductivity of 10 mS/m for both layers, a depth of 0.6 m for first the upper layer, and a depth of 1.2 m for the bottom layer. $EC_a$ data of the three consecutive years were inverted separately.

# Results and Discussion

## Calibration of EM38 Data using Soil $EC_{1:5}$

In this study, soil $EC_{1:5}$ was used as an indicator of soil salinity. Fig 2 shows the Pearson correlation coefficients between measured $EC_{1:5}$ and $EC_a$ from both EM38v and EM38h. Significant correlations are found between $EC_{1:5}$ and $EC_a$ for both EM38v and EM38h at different depths ($r > 0.90$, $P < 0.001$). According to Li et al. [19], the variation of soil salinity in the adjacent field of our study area was successfully characterized with $EC_a$ measurements from EM38h. Therefore, it was assumed that the variations of soil salinity (i.e. $EC_{1:5}$) in our study area can be solely explained by the variations of $EC_a$ values. Additionally, it is worth noting that the correlations between $EC_{1:5}$ and $EC_a$ from EM38h are higher than those between $EC_{1:5}$ and $EC_a$ from EM38v. Because the effective measuring depth of EM38h is approximately the rootzone, which is of great importance for studying the leaching process of salt, $EC_a$ measurements from EM38h were collected in the following years (i.e. 2009, 2010 and 2011) and used for characterization of spatio-temporal variations of soil salinity in the study area.

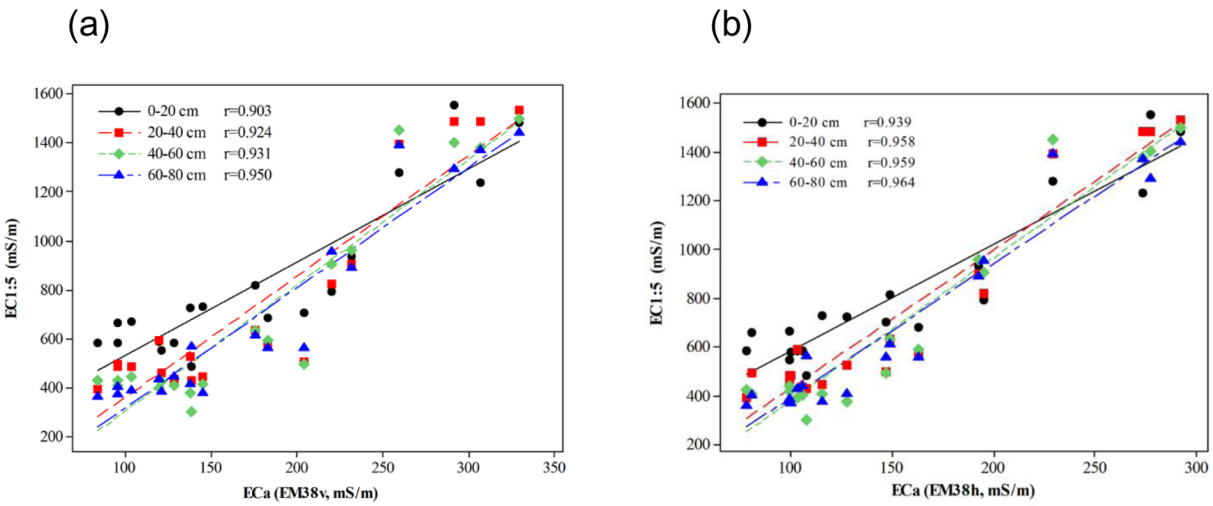


**Fig 2. Pearson correlation coefficients between soil $EC_{1:5}$ (mS/m) of the calibration points at various depths and $EC_a$ (mS/m) measurements with regard to EM38v (a) and EM38h (b).**

doi:10.1371/journal.pone.0127996.g002

## Statistical Analysis of Multi-Temporal EM38 Data

Table 1 shows basic summary statistics of measured $EC_a$ in 2009, 2010, and 2011. The average values decrease substantially from 2009 (166.19 mS/m) to 2010 (134.02 mS/m) and 2011 (113.29 mS/m). Similarly, the quartile estimates of $EC_a$ show a decreasing trend from 2009 to 2011. The Shapiro-Wilk statistics are 0.925, 0.930 and 0.925 with P-values less than 0.01, which indicate significant deviation from normality. In such cases, Box-Cox transformation method was used to transform the data by a monotonically increasing (or decreasing). In the next section, the datasets were normalized by this method.

Fig 3 shows the curves of the cumulative distribution function (CDF) for the study area which illustrates visible temporal variations of soil salinity among the three years. For a given $EC_a$ value, CDF is largest in 2011 and smallest in 2009. In order to quantify the difference, we used the Tukey-Kramer multiple comparison procedure. The values listed in Table 2 are the actual absolute differences in the means minus the least significant difference (i.e., abs-LSD). Positive abs-LSD values in Table 2 indicate significant difference ($P < 0.01$). It was found that the most significant change of $EC_a$ occurred between 2009 and 2011, followed by the period from 2009 to 2010, and then between 2010 and 2011.

## Characterizing Horizontal Spatio-Temporal Variability of Soil Salinity Using Geostatistical Approaches

Fig 4 shows the plot of experimental semivariances and the fitted semivariogram models for the $EC_a$ from 2009 to 2011. The parameters of these models are shown in Table 3. The semivariances of the models indicate that the spatial behavior has good continuity in space and can be

**Table 1. Descriptive statistics of $EC_a$ (mS/m) in 2009, 2010 and 2011.**

| Year | n | Mean | Stde | Min | 25% | Median | 75% | Max | Shapiro-Wilk Test |
|---|---|---|---|---|---|---|---|---|---|
| 2009 | 251 | 166.19 | 3.50 | 51.3 | 145.4 | 179.3 | 195.6 | 226.7 | 0.925 |
| 2010 | 256 | 134.02 | 2.00 | 20.1 | 96.15 | 151.85 | 182.9 | 217.7 | 0.930 |
| 2011 | 339 | 113.29 | 3.01 | 10.5 | 73.2 | 140.2 | 157.9 | 181.8 | 0.925 |

doi:10.1371/journal.pone.0127996.t001

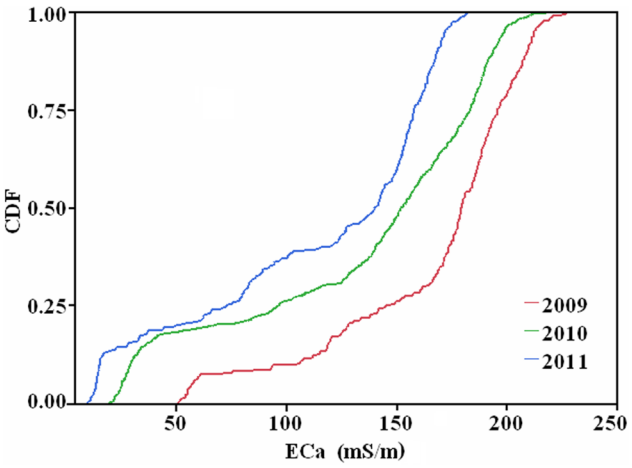


**Fig 3. Plot of cumulative distribution function (CDF) of $EC_a$ (mS/m) in 2009, 2010 and 2011.**

doi:10.1371/journal.pone.0127996.g003

modeled quite well with exponential models. However, different tendencies were found for models of the three years. The nugget value ($C_0$) decreases from 2009 to 2011, indicating that the variations of soil salinity over a short distance have become smaller and smaller. The ratios of $C_0$ to sill ($C+C_0$) decline sharply from 17.07% (2009) to 0.26% (2011). According to Shi et al. [36], a ratio less than 0.25 indicates strong spatial dependence; a value between 0.25 and 0.75 denotes moderate spatial dependence; and a value greater than 0.75 indicates weak spatial dependence. In this regard, we can conclude that the spatial autocorrelation of $EC_a$ was becoming stronger during the study period. This increase may be caused by the alternating irrigation and drainage practices necessary for rice cultivation. In addition, the relatively large nugget effect in the $EC_a$ data is most probably the consequence of an uneven distribution of soil salinity between ridge and furrow irrigation, perhaps associated with a small georeferencing error; Also the abrupt transitions in soil salinity, i.e. a short distance variability not to taken into account by the density of the sampling, and in this case, the nugget effect decreases, it can be assumed that the transitions, initially steep, soften between 2009 and 2011.

Maps of $EC_a$ in 2009, 2010, and 2011 generated by ordinary kriging are shown in Fig 5A, 5B and 5C, respectively. These maps show that $EC_a$ has decreased over the three years. For example, in a central block of the field (Easting: 286,520 m—286,560 m; Northing: 3,340,360 m—3,340,400 m) $EC_a$ was mostly larger than 200 mS/m in 2009, but the values decreased to175–200 mS/m in 2010 and then dropped to 125–150 mS/m in 2011.The decreasing ECa was most likely due to the irrigation and drainage practices for rice cultivation which leached the salts into a deep soil profile or the ground water.

The spatial distribution of soil salinity also changed. In 2009, the largest $EC_a$ values ($>$ 200 mS/m) were found in the center of the field and values decreased with distance from the center. However, in 2010 the largest $EC_a$ values ($>$ 200 mS/m) were found in the right half of the field and there was a distinctive difference in $EC_a$ between the left and right halves of the field. With

**Table 2. Comparison ofmeans of $EC_a$ (mS/m) for 2009, 2010, and 2011 using the Tukey-Kramer test.**

| Year | Mean | 2009 | 2010 | 2011 |
|---|---|---|---|---|
| 2009 | 166.19 | -11.61 | 22.71 | 42.06 |
| 2010 | 134.02 | | -6.64 | 12.24 |
| 2011 | 113.29 | | | -9.99 |

doi:10.1371/journal.pone.0127996.t002

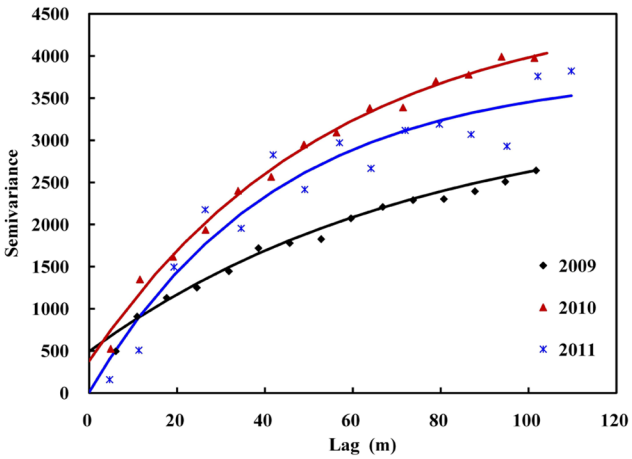


**Fig 4. Semivariance and fitted models (solid lines) for soil $EC_a$ (mS/m) from 2009 to 2011.**

doi:10.1371/journal.pone.0127996.g004

regard to year 2011, any differences in $EC_a$ between the left and right field halves were not obvious and the field was mostly dominated by $EC_a$ values of 125–150 mS/m. The heterogeneous and changing salinity distribution of the study area may be caused by the presence of ditches in the study area. Because the study area is a paddy field and surrounded by ditches (Fig 1C and 1D), it will be fully saturated with water during the crop cultivation, especially continuously irrigation and drainage made the salt wash away along with water in rice growth. Therefore, the rate of leaching of salts will be a function of the distance to the ditches. This is consistent with the large coefficient of variation ($CVt_i$) values in the margins of the study area shown in Fig 5D.

In order to quantify the temporal stability of salinity, $CVt_i$ values of each $EC_a$ measurement over three years are shown in Fig 5D. According to Shi et al. [36], the variation should be considered stable when $CVt_i$ is less than 10%, moderately stable when $CVt_i$ is between 10% and 25%, and unstable when $CVt_i$ is larger than 25%. Interestingly, the area with a high salinity content (Easting: 286,520 m—286,560 m; Northing: 3,340,400 m—3,340,440 m) displays temporal stability, while the surrounding area shows temporal instability, especially the edges of the field with a lower salinity level. This is consistent with the reports by Shi et al. [36]. The sharp change of salinity within the field edges may be due to the presence of irrigation ditches around the field where large amounts of irrigation water allow salts to leach into deeper soils.

## Mapping Vertical Spatio-Temporal Variation in Soil Salinity Using Quasi-3D Inversion

The Quasi-3D inversion results are shown in Fig 6. The vertical spatio-temporal variation of the soil salinity can be explained by the distribution of modeled σ. The soils in the study area were predicted to be inverted salinity profiles for all the three years. It was consistent with the calibration results shown in Fig 2. The widely distributed inverted salinity profiles were mostly

**Table 3. Models and parameters of semivariogram for ordinary kriging of soil $EC_a$ (mS/m) in 2009, 2010 and 2011.**

| Year | Semivariogram model | Nugget ($C_0$) | Sill ($C_0$+C) | $C_0$/($C_0$+C) | Range (A) | $r^2$ |
|---|---|---|---|---|---|---|
| 2009 | Exponential model | 495 | 2899 | 17.07 | 225.90 | 0.964 |
| 2010 | Exponential model | 380 | 4302 | 8.83 | 165.00 | 0.912 |
| 2011 | Exponential model | 10 | 3807 | 0.26 | 127.50 | 0.928 |

doi:10.1371/journal.pone.0127996.t003

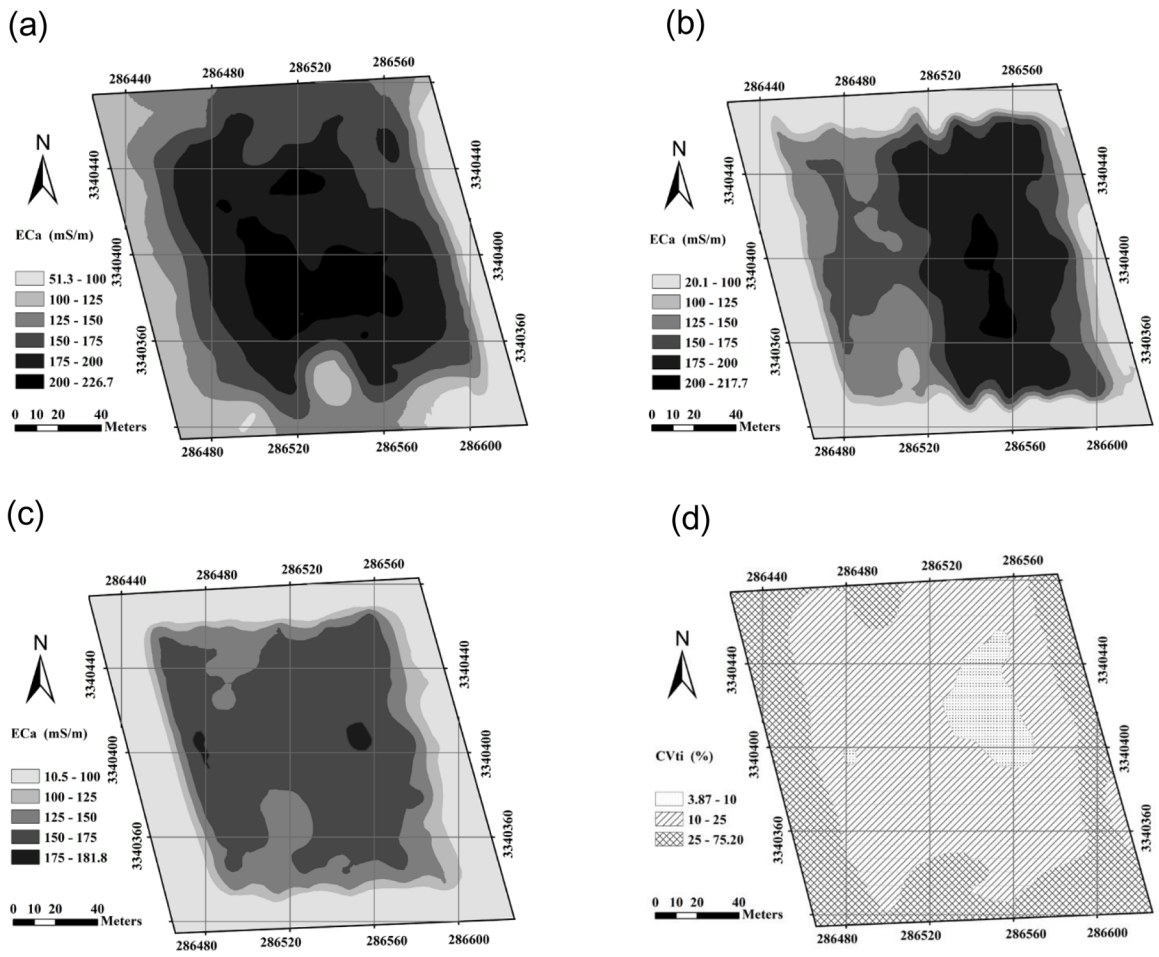


**Fig 5. Spatial distribution of soil $EC_a$ (mS/m) in (a) 2009, (b) 2010, and (c) 2011.** The plot of (d) coefficient of variation (*CVti*) over three years.

doi:10.1371/journal.pone.0127996.g005

likely caused by irrigation farming and high level of precipitation. Viewing from the 2-D cross-section oriented west-east, the salts of the soil migrate downwards over the three years. For example, the area with Eastings from 286,511.2 m to 286,545.6 m and depths from 0.5 m to 1.0 m was primarily dominated by σvalues between 150–200 mS/m in 2009. However, the conductivity of the area decreased to 100–175 mS/m in 2010. Furthermore, in the year of 2011 this conductivity was mostly between 100–125 mS/m. The decreasing distribution of soil salinity is also evident in 2-D cross-sections of the Quasi-3D models oriented south-north. The phenomenon is consistent with the vertical distribution of the soil salinity of paddy fields, whereby the salts will be washed out from the root zone over years of cultivation [19, 33]. The vertical distribution of salinity is also consistent with the annual precipitation of the study area (i.e., 1,300 mm). Additionally, the horizontal 2-D cross-sections at the top of the models for the three years are consistent with the kriging maps shown in Fig 5. This implies that the two approaches for determining spatio-temporal variation of salinity are reliable and consistent with each other.

## Conclusions

Repeated electromagnetic induction (EMI) surveys were carried out across a reclaimed paddy field in coastal regions of China over a three-year period. Significant correlation between apparent electrical conductivity ($EC_a$) and soil $EC_{1:5}$ ($r > 0.9$, $P < 0.001$) allowed for rapid

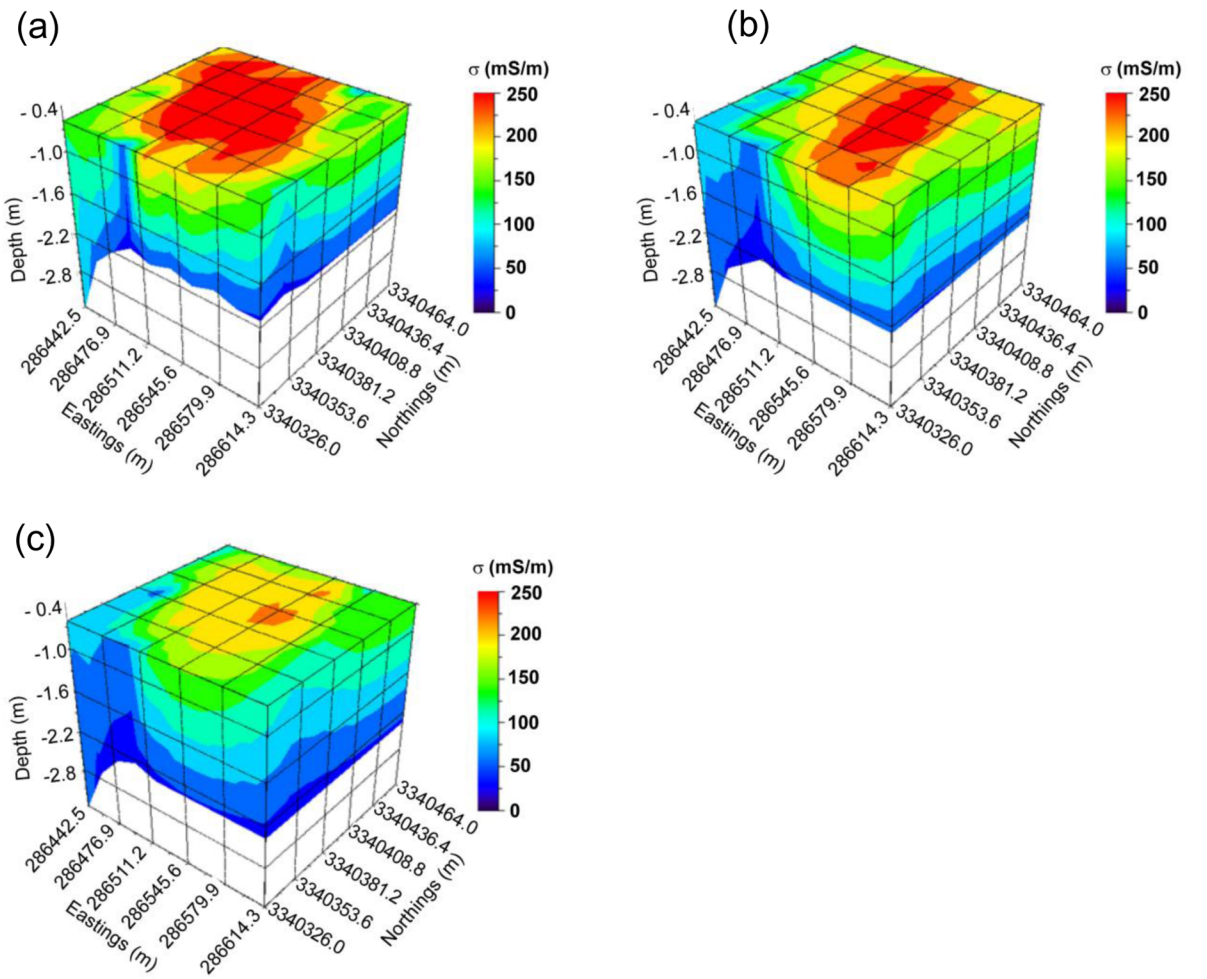


**Fig 6. Quasi-3D models of soil electrical conductivity (mS/m) in (a) 2009, (b) 2010 and (c) 2011 across the study area.**

doi:10.1371/journal.pone.0127996.g006

characterization of the spatio-temporal variation in soil salinity using $EC_a$ data. Ordinary kriging of $EC_a$ data showed the horizontal distribution of soil salinity was heterogeneous and the decrease of salinity may be a function of the distance to the irrigation ditches. Using a quasi-3D inversion approach, soils in the study areas were predicted to be inverted salinity profiles. The vertical leaching of salts with time was also successfully mapped, which was consistent with the location of irrigation ditches and high precipitation.

It is concluded that spatio-temporal variability of soil salinity in paddy fields can be characterized by the cost-effective and efficient EMI surveys. The methodology of this study can be used as guidance for researchers interested in understanding soil salinity development as well as land managers aiming for effective soil salinity monitoring and management practices. In order to better characterize the variations in soil salinity to a deeper soil profile, the deeper mode of EM38 (i.e., EM38v) as well as other EMI instruments (e.g. DUALEM-421) can be incorporated to conduct Quasi-3D inversions for deeper soil profiles [21, 37].

## Supporting Information

**S1 File. $EC_a$ measurements were harmonized onto a common grid consisting of the 251 $EC_a$ measurement sites in 2009 using the nearest neighbor algorithm available in ArcGIS**

**9.3 (ESRI, 2013).** 19 soil calibration points were sampled with recorded $EC_a$ measurements for the vertical (EM38v) and horizontal (EM38h) modes, respectively.
(XLSX)

## Acknowledgments

We thank Zhou Yin, Zhang Jiantao, Ji Wenjun for their assistance in the field-based measurements of paddy soil samples and Cheng Yongzheng, Wang Laigang for helpful comments on earlier versions of the manuscript.

## Author Contributions

Conceived and designed the experiments: YG ZS. Performed the experiments: YG ZS. Analyzed the data: YG JYH. Contributed reagents/materials/analysis tools: HYL. Wrote the paper: YG JYH.

## References

1. Huang MX, Shi Z, Gong JH (2008) Potential of multi-temporal ERS-2 SAR imagery for land use mapping in coastal zone of Shangyu city, China. Journal of Coastal Research 24: 170–176.
2. Yu TH, Shi CX, Wu YW, Shi MR (1996) Observation on salt spots in coastal land and study on tolerance of barley and cotton to Salt. Journal of Zhejiang Agricultural University 22: 201–204.
3. Doolittle JA, Brevik EC (2014) The use of electromagnetic induction techniques in soils studies. Geoderma 223– 225: 33–45.
4. Corwin DL (2008) Past, present, and future trends in soil electrical conductivity measurements using geophysical methods. InHandbook of Agricultural Geophysics; Allred B.J., Daniels J.J., Ehsani M.R. Eds., Raton Boca, Florida: CRC Press, Taylor and Francis Group. pp. 17–44.
5. Webster R, Oliver MA (1992) Sample adequately to estimate variograms of soil properties. Journal of Soil Science 43: 177–192.
6. Gallichand J, Buckland GD, Marcotte D, Hendry MJ (1992) Spatial interpolation of soil salinity and sodicity for a saline soil in Southern Alberta. Canadian Journal of Soil Science 72: 503–516.
7. Corwin DL, Rhoades JD (1982) An improved technique for determining soil electrical conductivity—depth relations from above ground electromagnetic induction measurements. Soil Science of Society America Journal 46: 517–520.
8. Corwin DL, Rhoades JD (1984) Measurements of inverted electrical conductivity profiles using electromagnetic induction. Soil Science of Society America Journal 48: 288–291.
9. Cook PG, Walker GR (1992) Depth profiles of electrical conductivity from linear combinations of electromagnetic induction measurements. Soil Science of Society America Journal 56: 1015–1022.
10. Lesch SM, Strauss DJ, Rhoades JD (1995) Spatial prediction of soil salinity using electromagnetic induction techniques. 1. Statistical prediction models: a comparison of multiple linear regression and cokriging. Water Resources Research 31: 373–386.
11. Lesch SM, Strauss DJ, Rhoades JD (1995) Spatial prediction of soil salinity using electromagnetic induction techniques. 2. An efficient spatial sampling algorithm suitable for multiple linear regression model identification and estimation. Water Resources Research 31: 387–398.
12. Padhi J, Misra RK (2011) Sensitivity of EM38 in determining soil water distribution in an irrigated wheat field. Soil &Tillage Research 117: 93–102.
13. Akramkhanov A, Martius C, Park SJ, Hendrickx JMH (2011) Environmental factors of spatial distribution of soil salinity on flat irrigated terrain. Geoderma 163: 55–62.
14. Triantafilis J, Laslett GM, McBratney AB (2000) Calibrating an electromagnetic induction instrument to measure salinity in soil under irrigated cotton. Soil Science of Society America Journal 64: 1009–1017.
15. Hendrickx JMH, Borchers B, Corwin DL, Lesch SM, Hilgendorf AC, Schlue J (2002) Inversion of soil conductivity profiles from electromagnetic induction measurements. Soil Science of Society America Journal 66: 673–685.
16. Monteiro Santos FA, Triantafilis J, Taylor RS, Holladay S, Bruzgulis KE (2010) Inversion of conductivity profiles from EM using full solution and a 1-D laterally constrained algorithm. Journal of Environmental & Engineering Geophysics 15: 163–174.

17. Mester A, van Der Kruk J, Zimmermann E, Vereecken H (2011) Quantitative two-layer conductivity inversion of multi-configuration electromagnetic induction measurements. Vadose Zone Journal 10: 1319–1330.
18. Viganotti M, Jackson R, Krahn H, Dyer M (2013) Geometric and frequency EMI sounding of estuarine earthen flood defence embankments in Ireland using 1D inversion models. Journal of Applied Geophysics 92: 110–120.
19. Li HY, Shi Z, Webster R, Triantafilis J (2013) Mapping the three-dimensional variation of soil salinity in a rice-paddy soil. Geoderma 195–196: 31–41. doi: 10.1093/jncimonographs/lgt025.Understanding PMID: 24395991
20. Shiraz FA, Ardejani FD, Moradzadeh A, Arab-Amiri AR (2013) Investigating the source of contaminated plumes downstream of the Alborz Sharghi coal washing plant using EM34 conductivity data VLF-EM and DC-resistivity geophysical methods. Exploration Geophysics 44: 16–24.
21. Triantafilis J, Ribeiro J, Page D, Monteiro Santos FA (2013)Inferring the location of preferential flow paths of a leachate plume by using a DUALEM-421 and a Quasi-Three-Dimensional inversion model. Vadose Zone Journal 12: 117–125.
22. Corwin DL, Lesch SM (2005) Characterizing soil spatial variability with apparent soil electrical conductivity: Part II. Case study. Computers and Electronics in Agriculture 46: 135–152.
23. Yao R, Yang JS (2010) Quantitative evaluation of soil salinity and its spatial distribution using electromagnetic induction method. Agricultural Water Management 97: 1961–1970.
24. Li HY, Webster R, Shi Z (2015) Mapping soil salinity in the Yangtze delta: REML and universal kriging (E-BLUP) revisited. Geoderma 237–238: 71–77.
25. Robinson DA, Lebron I, Lesch SM, Shouse P (2004) Minimizing drift in electrical conductivity measurements in high temperature environments using the EM-38. Soil Science of Society America Journal 68: 339–345.
26. Sheets KR, Hendrickx JMH (1995) Noninvasive soil water content measurement using electromagnetic induction. Water Resources Research 31: 2401–2409.
27. McNeill JD (1980) Electromagnetic terrain conductivity measurement at low induction numbers: Technical Note TN-6. GEONICS Limited Ontario Canada 15.
28. Corwin DL, Lesch SM (2003) Application of soil electrical conductivity to precision agriculture: theory principles and guidelines. Agronomy Journal 95: 455–471.
29. Li J, Heap AD (2011) A review of comparative studies of spatial interpolation methods in environmental sciences: Performance and impact factors. Ecological Informatics 6: 228–241.
30. Webster R, Oliver MA (2007) Geostatistics for Environmental Scientists, 2nd. England: John Wiley & Sons.
31. Blackmore S (2000) The interpretation of trends from multiple yield maps. Computers and Electronics in Agriculture 26: 37–51.
32. Shi Z, Wang K, Bailey JS, Jordan C, Higgins AH (2002) Temporal changes in the spatial distribution of some soil properties on a temperate grassland site. Soil Use and Management 18: 353–362.
33. Monteiro Santos FA, Triantafilis J, Bruzgulis K (2011) A spatially constrained 1D inversion algorithm for quasi-3D conductivity imaging: application to DUALEM-421 data collected in a riverine plain. Geophysics 76: B43–B53.
34. Sasaki Y (1989) Two-dimensional joint inversion of magnetotelluric and dipole-dipole resistivity data. Geophysics 54: 254–262.
35. DeGroot-Hedlin C, Constable SC (1990) Occam's inversion to generate smooth two-dimensional models from magnetotelluric data. Geophysics 55: 1613–1624.
36. Shi Z, Li Y, Wang RC, Makeschine F (2005) Assessment of temporal and spatial variability of soil salinity in a coastal saline field. Environmental Geology 48: 171–178.
37. Huang JY, Davies GB, Bowd D, Monteiro Santos FA, Triantafilis J (2014) Spatial prediction of exchangeable sodium percentage at multiple depths using electromagnetic inversion modelling. Soil Use and Management 30: 241–250.